Practical Laboratory Medicine 35 (2023) e00314

Contents lists available at ScienceDirect

Practical Laboratory Medicine

journal homepage: www.elsevier.com/locate/plabm

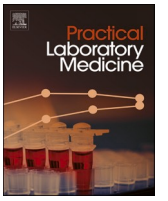

Development of a quantitative fluorescence lateral flow immunoassay (LFIA) prototype for point-of-need detection of anti-Müllerian hormone

Heather J. Goux [a], Binh V. Vu [b], Katherine Wasden [b], Kannan Alpadi [c], Ajay Kumar [c], Bhanu Kalra [c], Gopal Savjani [c], Kristen Brosamer [d], Katerina Kourentzi [b,*], Richard C. Willson [a,b,d,e,**]

[a] Department of Biology and Biochemistry, University of Houston, Houston, TX, USA
[b] William A. Brookshire Department of Chemical and Biomolecular Engineering, University of Houston, Houston, TX, USA
[c] Ansh Labs, Webster, TX, USA
[d] Department of Biomedical Engineering, University of Houston, Houston, TX, USA
[e] Escuela de Medicina y Ciencias de la Salud, Tecnológico de Monterrey, Monterrey, Nuevo León, Mexico

ARTICLE INFO

Keywords:
Lateral flow assay
Europium reporters
Antibody
Fluorescence
Biomarker
Quantitative
Anti-Müllerian Hormone
Point-of-need

ABSTRACT

Objective: Anti-Müllerian Hormone (AMH) is a quantitative marker for ovarian reserve and is used to predict response during ovarian stimulation. Streamlining testing to the clinic or even to the physician's office would reduce inconvenience, turnaround time, patient stress and potentially also the total cost of testing, allowing for more frequent monitoring. In this paper, AMH is used as a model biomarker to describe the rational development and optimization of sensitive, quantitative, clinic-based rapid diagnostic tests.

Design and Methods: We developed a one-step lateral-flow europium (III) chelate-based fluorescent immunoassay (LFIA) for the detection of AMH on a portable fluorescent reader, optimizing the capture/detection antibodies, running buffer, and reporter conjugates.

Results: A panel of commercial calibrators was used to develop a standard curve to determine the analytical sensitivity (LOD = 0.41 ng/ml) and the analytical range (0.41–15.6 ng/ml) of the LFIA. Commercial controls were then tested to perform an initial evaluation of the prototype performance and showed a high degree of precision (Control I CV 2.18%; Control II CV 3.61%) and accuracy (Control I recovery 126%; Control II recovery 103%). *Conclusions*: This initial evaluation suggests that, in future clinical testing, the AMH LFIA will likely have the capability of distinguishing women with low ovarian reserve (<1 ng/ml AMH) from women with normal (1–4 ng/ml AMH) ovarian reserve. Furthermore, the LFIA demonstrated a wide linear range, indicating the assay's applicability to the detection of other health conditions such as PCOS, which requires AMH measurement at higher concentrations (>6 ng/ml).

* Corresponding author. University of Houston, William A. Brookshire Department of Chemical & Biomolecular Engineering, 4226 Martin Luther King Blvd., Houston, TX, 77204, USA.

** Corresponding author. University of Houston, William A. Brookshire Department of Chemical & Biomolecular Engineering, 4226 Martin Luther King Blvd., Houston, TX, 77204, USA.

E-mail addresses: edkourentzi@uh.edu (K. Kourentzi), willson@uh.edu (R.C. Willson).

https://doi.org/10.1016/j.plabm.2023.e00314
Received 13 October 2022; Received in revised form 27 February 2023; Accepted 12 April 2023
Available online 13 April 2023

1. Background

Anti-Müllerian hormone (AMH), a dimeric glycoprotein belonging to the transforming growth factor-β (TGF-β) superfamily, is a standard quantitative marker of ovarian reserve used to predict response during ovarian stimulation and often measured during assisted reproductive treatments [1,2]. Unlike other fertility markers such as follicle-stimulating hormone (FSH) and luteinizing hormone (LH), AMH can be measured at any time during a woman's monthly cycle, making it a valuable tool for assessing fertility in women.

Nine percent of couples, 48.5 million couples worldwide, experience infertility and many resort to *in vitro* fertilization (IVF), in preparation for which serum AMH levels are measured in an effort to predict the chances of conception with IVF. In addition to monitoring ovarian reserve, AMH can be used in the diagnosis of a variety of ovarian diseases including primary ovarian insufficiency, oncofertility, gonadotoxicity, premature ovarian aging, polycystic ovarian syndrome, and cryptorchidism, and also for assessment of testicular function [1–5].

Current testing for AMH often requires shipping blood or serum samples to a central laboratory to be analyzed using an enzyme-linked immunosorbent assay [6] (AMH Gen II ELISA), with a relatively long turnaround time of about two days [7]. Significant inter-laboratory and inter-assay variation in AMH ELISAs has been reported [8,9]. Moreover, there has been a question of the stability of AMH during storage/transport, which also might affect measured serum AMH values [2,10,11] and of the general utility of a single measurement for reliable clinical decisions due to AMH level fluctuations during a normal cycle [12]. Streamlining AMH testing (and other hormonal assays used in combination with AMH to provide reliable ovarian reserve estimates) to a patient's physician's office would reduce inconvenience, turnaround time, patient stress and potentially also the total cost of testing, allowing for increased patient awareness [13] and more frequent monitoring.

Lateral Flow Immunoassays (LFIAs), popularized by the over-the-counter pregnancy test and more recently the rapid COVID-19 antigen test, are a standard format for point-of-care tests, as they fulfill all of the WHO "ASSURED" (Affordable, Sensitive, Specific, User-friendly, Rapid and Robust, Equipment-free and Deliverable to end-users) usability criteria. They address many technical challenges associated with point-of-care testing in resource-limited settings, e.g. a general care physician's office or at home [14,15]. They can eliminate the need for complex/expensive instruments, use lyophilized reagents ensuring long-term stability without refrigeration, use minimally-invasive samples (e.g. saliva, urine, fingerstick blood), have relatively simple procedures for ease-of-use by minimally-trained operators, and have a stand-alone capability that makes this platform practical for rapid on-site measurements.

A typical LFIA consists of a nitrocellulose membrane along which the sample wicks from the sample application zone to a detection zone, continuing until it reaches the absorbent pad. In the detection zone, the reporter-bound analyte is captured by a target-specific affinity reagent immobilized at the test line. Further downstream of the test line is the control line, which is composed of an affinity reagent which directly captures the reporter conjugate. A signal generated at the test line signifies a positive result, while a signal generated at the control line confirms that the test was performed properly.

For an AMH LFIA to be clinically relevant, it must be able to accurately distinguish between a woman with a low ovarian reserve and a woman with normal ovarian reserve. Healthy women under the age of 30 have an estimated AMH level ranging from 1.8 to 4.8 ng/ml [16,17] and AMH average levels steadily decrease to 0.25–1.2 ng/ml for women above the age of 42. Historically an AMH level of 1 ng/ml has been considered as the threshold cut-off for low ovarian reserve, as women with ≤ 1 ng/ml of AMH typically respond poorly to controlled ovarian stimulation (COS) [17–19] (the more recent Poseidon classification uses 1.3 ng/ml and the previously-used Bologna classification used a range, 0.5–1.1 ng/ml [20,21]) and an AMH level <0.7 ng/ml predicts a poor response to COS especially with advanced age [18]. Notably, poor *in vitro* fertilization results were observed in women with AMH between 0.1 and 0.5 ng/ml, suggesting limited additional clinical value of LOD below 0.5 ng/ml [18].The ubiquitous gold nanoparticle LFIA is generally not quantitative (nearly all quantitative LFAs are based on light-emitting labels [22,23]) and has a typical LOD in the range of 2–5 ng/ml [24,25].

Fluorescent europium chelate nanoparticles used as reporters in LFIAs allow quantitative measurements [26] and have been shown to be up to 300-fold more sensitive than typical colloidal gold reporter particles [24]. Europium microspheres are excited at 365 nm and emit at 610 nm. With the appropriate emission filter, this substantial Stokes shift allows for effective isolation of the emitted luminescent signal. Additionally, europium (III) has a decay time (>500 μs) that far exceeds the decay times of other fluorescent emitters (<50 ns) and therefore can serve as the basis of time-resolved fluorescence-based immunoassays. Several low-cost, POC-ready readers are available for unbiased reading and quantification of europium-based LFIAs. Here we report the design and methodical development of a reader-based fluorescence Lateral Flow Immunoassay (LFIA) prototype using commercially-available europium chelate FluoSpheres as reporters for the quantitative detection of AMH. Moreover, because the development of LFIAs is typically empirical and takes place in proprietary settings, we provide detailed protocols to facilitate broad adoption of europium-based LFIAs by others in the field.

2. Materials and methods

2.1. AMH standards

Ansh Labs (Webster, TX) provided the calibrators and controls used in this work. Recombinant pro-mature form AMH (the content of AMH/MIS Calibrator Set [B–F] and Control Set; received lyophilized) was standardized with a purified recombinant mature AMH preparation that was characterized by mass spectrometry and optical absorbance (280 nm). Upon arrival, the lyophilized standards were reconstituted in 1 ml DI water, aliquoted, and stored at -20 °C. AMH/MIS Calibrator A (a protein-based buffer supplemented

with 0.05% Pro-Clean 400 5-chloro-2-methyl-4-isothiazolin-3-one, containing no AMH) was used as the sample diluent.

AMH LFIA optimization experiments used AMH/MIS Calibrator F (lot no. 120417; 14.2 ng/ml AMH) as the AMH standard. The AMH/MIS Calibrator Set [A-F] (cat no. AMH/MIS- CAL-105-Set; lot no. 120417; 0–15.6 ng/ml AMH) was used to generate calibration curves to determine the limit of detection (LOD) of the AMH LFIA. In addition to serving as a negative control, Calibrator A (0 ng/ml AMH) was also used as a diluent to expand the range of the calibration curve. Specifically, a 1:3 ratio of Calibrator A to Calibrator B was used to make Calibrator B/3. AMH/MIS Control Set (cat no. AL-CTR-105-SET, lot no. 120417-2020-12-03) was used to determine the precision and accuracy of the AMH LFIA.

2.2. Biotinylated anti-AMH antibodies

Monoclonal mouse anti-AMH antibodies (Ansh Labs, cat no. AB-303-AA0011, AB-303-AA0012, and AB-303-AA0024) were biotinylated using the EZ-Link Sulfo–NHS–LC-Biotin reagent (Thermo Fisher Scientific; cat no. 21335; Waltham, MA), following the manufacturer's protocol. A 20-fold molar excess of biotin reagent was used to label 50 μg of monoclonal anti-AMH antibody. The reaction was incubated for 30 min at room temperature (RT). The excess non-reacted and hydrolyzed biotin reagent was removed from the labeled protein using a Zeba desalting column (Thermo Fisher Scientific; 7 K MWCO, 0.5 ml; Waltham, MA), and the final product was stored at 4 °C in PBS buffer (pH 7.4).

2.3. Coupling of anti-AMH antibodies to Eu (III) FluoSpheres

100 μl of $1x10^{12}$ particles/ml (0.5%) of 0.2 μm FluoSpheres carboxylate-modified europium (III) microspheres (excitation at 365 nm; emission at 610 nm; Thermo Fisher Scientific; cat no. F20881) were sonicated for 5 min using a Fisher Scientific FS30 Ultrasonic Cleaner. To wash particles, the suspension was centrifuged at 15,000×*g* for 10 min. The supernatant was removed, and particles were resuspended in 300 μl of 50 mM MES buffer (pH 5.8) and sonicated for 3 min. After two rounds of washing, the microspheres were resuspended in 95 μl of 50 mM MES, pH 5.8. Then 3 μl of 10 mg/ml 1-Ethyl-3-(3-dimethylaminopropyl) carbodiimide (EDC) and 2.0 μl of 5 mg/ml N-Hydroxysuccinimide (NHS) were added to the microsphere suspension and incubated for 30 min on a rotator at room temperature. The microspheres were then washed in 1 ml of PBS (pH 7.4) to remove the activation solution and resuspended in 300 μl of PBS (pH 7.4). The particles were vortexed and sonicated (3 min) to remove any aggregates, and 35 μg of anti-AMH detection antibody (44 μl of the 0.8 mg/ml stock solution of AB-303-AA0011 or 17.5 μl of the 2 mg/ml stock solution of AB-303-AA0012) were added. The mixture was placed on a rotator for 4 h at RT. After incubation, the anti-AMH antibody microsphere conjugates were centrifuged at 15,000×*g* for 10 min, resuspended in 300 μl of PBS with 4% BSA (bovine serum albumin), sonicated for 3 min and placed on a rotator for 30 min at RT. The anti-AMH antibody microsphere conjugates were then washed three times by centrifugation at 15,000×*g* for 10 min, resuspending the pellet in 1 ml of PBS, and sonicating the resuspended particles for 3 min. Anti-AMH antibody microsphere conjugates were finally resuspended in 100 μl of PBS (10^{12} microspheres/ml) and stored at 4 °C.

2.4. AMH LFIA dipstick

3-mm wide lateral flow dipsticks were prepared, consisting of a 30-mm long Whatman GE Healthcare (Pittsburgh, PA) FF80HP nitrocellulose membrane, a 22-mm long Whatman GE Healthcare CF5 absorbent pad, and an adhesive backing card (DCN Diagnostics; cat no. MIBA-020; Carlsbad, CA). Test and control lines were generated on the nitrocellulose membrane using a Lateral Flow Reagent Dispenser (Claremont BioSolutions; Upland, CA) and a Fusion 200 syringe pump (Chemyx, Inc.; Stafford, TX) with a flow rate of 0.22 ml/min and 4 cm/s head speed. Mouse anti-AMH monoclonal capture antibodies (Ansh Labs; cat no. AB-303-AA0024) were diluted to 1 mg/ml in PBS buffer (pH 7.4) and applied to the membrane 7 mm from the end of the absorbent pad to make the test line. Goat anti-mouse IgG antibodies (Arista Biological Inc.; cat no. ABGAM-0500; Allentown, PA) were diluted to 1 mg/ml in PBS buffer (pH 7.4) and dispensed on the membrane to make the control line, 2 mm from the absorbent pad.

2.5. Screening of LFIA running buffers

Several buffers were tested during optimization: Buffer 1 contained BlockAid™ blocking solution (Thermo Fisher Scientific, cat no. B10710), composed of a proprietary formulation of proteins in PBS buffer, pH 7 with 0.02% thimerosal. Buffer 2 contained PBS (140 mM NaCl, 2.7 mM KCl, 10 mM PO_4^{3-}), 1% BSA (Sigma-Aldrich, cat. no A7906; St. Louis, MO), and 0.5% Tween 20. Buffer 3 contained PBS buffer (140 mM NaCl, 2.7 mM KCl, 10 mM PO_4^{3-}), 1% (v/v) Tween 20, 1% (v/v) Triton X-100, and 0.5% (w/v) 3350 g/mol polyethylene glycol (PEG). Buffer 4 contained 10 mM HEPES, 25 mM NaCl, 0.3% 3350 PEG, 1% Tween 20, and 0.5% (w/v) non-fat dried milk (NFDM), pH 8. PBS tablets were from Takara Bio USA Inc. (pH 7.4; cat no. T9181; Mountain View, CA). All other reagents were of analytical grade and purchased from Sigma-Aldrich (St. Louis, MO).

2.6. AMH LFIA

The stock solution of anti-AMH microsphere conjugate ($1x10^{12}$ particles/ml) was sonicated (5 min), vortexed, and diluted 10-fold in the optimized running buffer (PBS buffer (140 mM NaCl, 2.7 mM KCl, 10 mM PO_4^{3-}), 1% BSA, 0.5% Tween 20). After dilution, the anti-AMH microsphere conjugate suspension was again sonicated (15 min) and vortexed to prevent the formation of aggregates. The AMH LFIA dipstick was inserted into an Eppendorf tube containing 10 μl of the diluted anti-AMH microsphere conjugate stock (10^9

particles/reaction) and 40 μl of sample. After 20 min, the dipsticks were removed from the tubes, and imaged and analyzed using the ESEQuant LR3 system (Qiagen Lake Constance; Stockach, Germany). The AMH LFIA workflow is shown in Fig. 1.

2.7. Dipstick imaging and analysis

Fluorescent AMH dipsticks were read with the portable, standalone ESEQuant LR3 Lateral Flow reader (Qiagen) equipped with a drawer adaptable to LFA dipsticks of different widths. Lateral Flow Studio software (Qiagen) was used to set the scanning range and wavelengths (channel E1/D1; excitation at 365 nm and emission at 610 nm), and to initiate scans. Once a raw emission scan was acquired, it was directly uploaded and viewed on a PC with Lateral Flow Studio to locate the test and control lines. The optical densities (OD, peak area) of the test line (TL) and control line (CL) were measured to calculate the ratio of TL to CL ($\frac{TL}{CL}$; AMH LFIA signal).

A FluorChem-based laboratory imaging platform was also used to image the dipsticks during AMH LFIA optimization. The FluorChem platform comprised a FluorChem SP gel cabinet (Alpha Innotech Corp., San Leandro, CA), stacked SYPRO Orange (595 nm ± 40) filter and Quantaray YA2 58 mm filter, a built-in reflective UV lamp, and a CoolSNAP K4 CCD 2048 × 2048-pixel camera (Photometrics, Blaine WA) and was controlled by Micro-Manager 1.4.22 software (Vale Lab, University of California, San Francisco, CA).

ImageJ version 1.8.0_112 (Rasband Lab, U. S. National Institutes of Health, Bethesda, MD) was used to analyze the dipstick images. Before image analysis, a spatial calibration was performed to set the number of pixels across the width of the LFIA strip (3 mm). A plot profile of pixel intensities as a function of position along the membrane was generated. A line was drawn between valleys on the plot to allow the area under the peaks to be integrated. The areas under the curves located at the regions of the test and control lines were defined as the test line signal (TL) and the control line signal (CL), respectively. The test output was then calculated as the ratio of TL to CL signals ($\frac{TL}{CL}$).

3. Results

3.1. Antibody optimization

We chose three ELISA-validated mouse monoclonal antibodies (Ansh Labs, cat no. AB-303-AA0011, AB-303-AA0012, and AB-303-AA0024) to develop the AMH LFIA. These antibodies target linear epitopes on the associated homodimer of AMH (binding targets of commercial mAbs are at http://www.globalbiotec.co.th/attachments/view/?attach_id=56451) (Fig. 2). The non-covalently associated pro-mature homodimer of AMH has been previously identified to be the biologically active form and therefore the most clinically-relevant form of the hormone [27].

ELISA-validated antibodies must be re-evaluated for use in a lateral-flow format, as absolute and relative performance can vary when transitioning from a plate-based ELISA to a lateral flow assay [28]. ELISA performance is typically governed by a slow kinetic dissociation rate (k_{off}), while LFIA performance may be maximized by a fast association rate (k_{on}). Furthermore, an ELISA includes several rounds of washing to remove non-specifically bound detection antibodies. In an LFIA, the capacity of the absorbent pad restricts the volume of washing, and avoidance of a separate washing step is usually preferable for convenience and rapid time-to-result. Hence, achieving high sensitivity in a lateral flow assay requires an antibody pair with minimal non-specific binding and high k_{on}. The candidate antibodies were tested in different orientations and combinations in a streptavidin gold nanoparticle (DCN; cat no. PACG) LFIA to determine the optimal capture and detection antibodies for AMH LFA. The streptavidin-biotin system is commonly used to screen antibodies due to its simplicity and the possibility for all detection mAbs to share a single, common reporter. Antibodies were biotinylated (see protocol in Material and Methods) and then coupled to the streptavidin gold reporter particles.

All possible combinations of mAbs were tested in both positive and no-target (negative) reactions. Positive and no-target reactions contained 20 μl of standard (14.2 ng/ml of AMH) and 20 μl PBS buffer respectively, along with 2 μl of the biotinylated antibody (0.1 μg/μl in PBS, pH 7.4), 10 μl of 40 nm Streptavidin gold nanoparticles (10^9 particles/reaction), and 20 μl of PBS, 1% BSA, pH 7.4. Each capture mAb was spotted (1 μl, 0.4 μg/μl in PBS) on dipstick nitrocellulose strips at 7 mm from the control line and dried at 37 °C for 20 min. Dipsticks were added to reactions and incubated for 30 min before an additional 50 μl of PBS, 1% BSA, pH 7.4 was added. After 1 h, the gold nanoparticle dipsticks were removed from the reaction tubes and scanned on a Perfection V600 flatbed color scanner (Epson; Long Beach, CA). ImageJ software was used to analyze images. We defined the areas of the peaks located at the test line and the

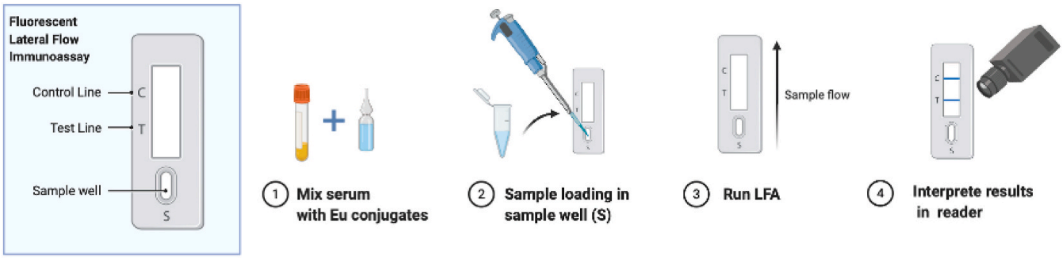

Fig. 1. Anti-Müllerian hormone (AMH) LFIA workflow. Created with Biorender.com.

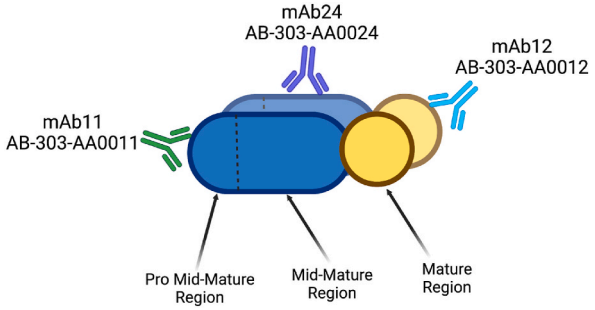

Fig. 2. Anti-Müllerian hormone (AMH) as it exists in its biologically active form, as a non-covalently associated pro-mature homodimer including the binding sites of the candidate anti-AMH monoclonal antibodies (mAbs). mAbs AB-303-AA0011 (isotype IgG2b; green Y), AB-303-AA0012 (isotype IgG1; blue Y), and AB-303-AA0024 (isotype IgG2b; purple Y) bind to the Pro-mid-mature, the Mature region, and the Mid-mature region on the pro-mature form of AMH, respectively. The dotted line indicates the eventual cleavage site and the dissociation of the pro-N-terminal and the mature C-terminal regions. Created with Biorender.com. (For interpretation of the references to color in this figure legend, the reader is referred to the Web version of this article.)

control line as the test line signal (TL) and the control line signal (CL), respectively. The output for each test was defined as the ratio of TL to CL signals ($\frac{TL}{CL}$).

Antibody target-specific binding was defined as the difference in average $\frac{TL}{CL}$ ($\Delta\frac{TL}{CL}$; Table 1; purple color) between positive reactions (blue color, Table 1; n = 1; Table 1; red color). A low background signal ($\frac{TL}{CL}$ of the negative control) and high target-specific binding are equally important during lateral flow immunoassay development. Antibody pairs that included mAb AB-303-AA0024 as the capture antibody produced the highest target-specific binding. Antibody AB-303-AA0024 was therefore chosen as the capture antibody at the test line for AMH detection in the LFIA in all following experiments. Of all antibody pairs, the mAb AB-303-AA0024 (capture)/biotinylated mAb AB-303-AA0012 (bio12; detection) pair had the highest target-specific binding ($\Delta\frac{TL}{CL} = 1.59$)

Table 1
Screening of antibodies for detection of AMH in lateral flow.

		Detection mAb			
		bio11	bio12	bio24	AMH (ng/ml)
Capture mAb	11	**0.95**	**0.21**	**0.45**	14.2
		0.30	**0.10**	**0.05**	0
	12	**0.03**	**0.07**	**0.18**	14.2
		0.02	**0.08**	**0.06**	0
	24	**2.46**	**1.10**	**0.61**	14.2
		0.86	**0.27**	**0.20**	0

		Detection mAb		
		bio11	bio12	bio24
Capture mAb	11	**0.65**	**0.12**	**0.40**
	12	**0.01**	**0.00**	**0.12**
	24	**1.59**	**0.84**	**0.41**

and background signal ($\Delta \frac{TL}{CL} = 0.86$). mAb AB-303-AA0024 (capture)/biotinylated mAb AB-303-AA0011 (bio11; detection) pair showed a large drop in target-specific binding ($\Delta \frac{TL}{CL} = 0.84$) and background signal ($\frac{TL}{CL} = 0.27$). As expected, using the same monoclonal antibody for both capture and detection showed very low target-specific binding with respect to the background signal. Under initial screening conditions, no antibody pair showed both superior target-specific binding and low background signal, and thus we proceeded with AMH LFIA optimization using both the 24/12 and the 24/11 antibody pairs.

In the upper table, the intensity of the blue color in odd-numbered lines denotes test output (the ratio of signal intensities at the test and control lines; $\frac{TL}{CL}$) with 14.2 ng/ml of AMH, and the intensity of the red color in even-numbered rows denotes the non-specific background signal with no AMH. In the lower table, the intensity of the purple color indicates the degree of target-specific binding defined as the difference in signals ($\Delta \frac{TL}{CL}$) with 14.2 ng/ml and zero AMH.

3.2. LFIA buffer screening

Running buffer components can be varied to improve target-specific binding of reporters and suppress non-specific binding. Surfactants and polymers are effective in suppressing aggregation, and surfactants and blocking agents can reduce non-specific binding. Varying pH and salt concentrations can affect antibody affinity. We selected four buffers that varied widely in the types and concentrations of each of these components. These four buffers were tested in the streptavidin gold nanoparticle AMH LFIA in both positive and no-target AMH reactions and assessed by their effect on target-specific binding ($\Delta \frac{TL}{CL}$).

The reaction tubes contained 20 μl of AMH standard or PBS buffer, 2 μl of biotinylated mAb AB-303-AA0011 (0.1 ng/μl; PBS, pH 7.4), 10 μl of 40 nm streptavidin-gold nanoparticles (1x 10^9 particles/reaction), and 20 μl of Buffer 1, 2, 3, or 4. Dipsticks were added to reaction tubes and incubated for 30 min before the addition of 50 μl of the corresponding buffer (1, 2, 3, or 4). After 20 min, dipsticks were removed and scanned on a Perfection V600 flatbed color scanner, and images analyzed using ImageJ software.

In the screening gold LFA, reactions using Buffer 2 had the highest mAb/AMH target-specific signal ($\Delta \frac{TL}{CL} = 0.4$), approximately two-fold higher than the reactions based on Buffers 1 or 4. Buffer 3 adversely affected mAb/AMH target-specific binding ($\Delta \frac{TL}{CL} =$ -0.48), causing a larger $\frac{TL}{CL}$ in the no-target reaction than in the positive reactions. Buffer 2 was chosen as the best AMH LFIA running buffer and used in the remainder of the study.

3.3. Europium (III) chelate luminescent nanoparticle reporters

For an AMH LFIA to be clinically relevant, it must quantitatively distinguish between women with low and normal ovarian reserve. Healthy women under the age of 35 have an AMH level that ranges from 1.5 to 4 ng/ml, lower than the typical sensitivity of conventional gold nanoparticle LFIAs, which normally also are not sufficiently quantitative. FluoSpheres™ europium (III) nanoparticles are commercially-available polystyrene nanoparticles containing europium chelates featuring a narrow long-wavelength emission peak (610 nm) well-separated from the excitation peak (365 nm). This large Stokes shift allows the effective use of simple filters to selectively detect the europium emission signal. Eu nanoparticles have been used as fluorescent reporters in LFIAs and shown to be up to 300-fold more sensitive than typical colloidal gold particles, and to support quantitative LFIAs.

We initially tested NeutrAvidin-labeled FluoSpheres europium microspheres (0.2 μm, Thermo Fisher Scientific, cat. no F20884) labeled with biotinylated anti-AMH antibodies, but the observed LFIA sensitivity was not in the useful range. We then tested covalent antibody coupling by carbodiimide chemistry to carboxylate-modified FluoSpheres europium microspheres (0.2 μm, Thermo Fisher Scientific, cat. no F20881). We optimized the activation protocol and finally used a 3-fold molar excess of EDC and a 20-fold molar excess of NHS (with respect to the total surface carboxylate groups) to minimize particle aggregation. One antibody monolayer (estimated based on the studies of polystyrene particle capacity reported in Osborne et al. [29]) equivalent was offered, and we

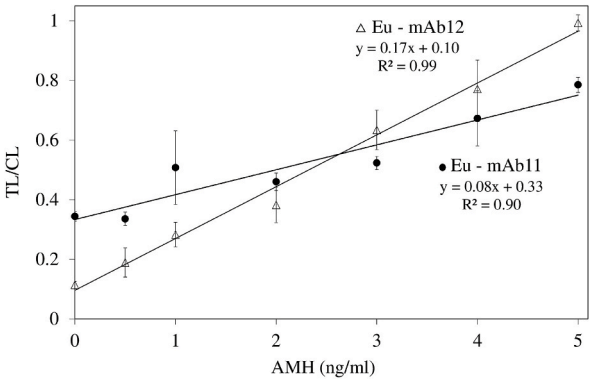

Fig. 3. AMH LFIA standard curves using reporters conjugated with different antibodies. The average $\frac{TL}{CL}$ signal from dipsticks (containing capture mAb24 on the test line) tested with dilutions of AMH standard (0–5 ng/ml) and 10^9 Eu particles functionalized with antibody AB-303-AA0011 (●; n = 5) or antibody AB-303-AA0012 (△; n = 5).

prepared LFIA reporter particles by directly coupling the two different detection antibodies (mAb AB-303-AA0011 and mAb AB-303-AA0012). We evaluated and compared the effect of these reporter conjugates on AMH LFIA sensitivity and background signal.

The commercial AMH standard (14.2 ng/ml) was used to make serial dilutions (0–5 ng/ml) in PBS pH 7.4, 1% BSA. Reaction mixtures contained 40 µl of AMH dilution and 10 µl (10^9 particles/reaction) mAb AB-303-AA0011 or mAb AB-303-AA0012 microsphere conjugates (n = 5). Dipsticks were imaged on the FluorChem device (using an exposure time of 250 ms and a binning of 2) and images analyzed with ImageJ.

The average $\frac{TL}{CL}$ generated from the no-target (0 ng/ml of AMH) negative control reactions (background) was higher with the mAb AB-303-AA0011 reporter conjugates (average $\frac{TL}{CL} = 0.38$) than with mAb AB-303-AA0012 reporter conjugates (average $\frac{TL}{CL} = 0.11$) (Fig. 3). Antibody target-specific binding, defined as the average difference in test output ($\Delta \frac{TL}{CL}$) between reactions with 5 ng/ml and 0 ng/ml of AMH (no-target reactions) was higher when mAb AB-303-AA0012 was used rather than mAb AB-303-AA0011. Therefore, mAb AB-303-AA0012 europium microspheres were chosen as the AMH LFIA reporter used in further studies.

3.4. Lateral flow immunoassay membrane

A dilution series of AMH standards (0–2 ng/ml of AMH) in PBS, 1% BSA, 0.5% Tween 20 was used to test nitrocellulose dipsticks of three different compositions (Membrane A: Whatman GE Healthcare FF80HP; Membrane B: Sartorius Stedim Biotech UniSart CN 95; Membrane C: Millipore HiFlow 90). Reaction mixtures containing 40 µl of each sample dilution and 10 µl of anti-AMH mAb AB-303-AA0012 Eu microsphere conjugates (10^9 particles/reaction), were incubated for 30 min before the addition of the dipsticks. The dipsticks were then imaged all together on the FluorChem device (250 ms exposure; binning of 2x2) and analyzed with ImageJ.

We evaluated the different membranes for their effect on the background signal and AMH detection sensitivity. All three nitrocellulose membranes produced a similar low level of non-specific binding; all no-target (0 ng/ml of AMH) reactions had an output ($\frac{TL}{CL}$) < 0.02 (Fig. 4). Membrane A dipsticks consistently demonstrated the highest target-specific binding ($\frac{TL}{CL}$) over the whole AMH dilution series. As a result, Membrane A was chosen as the lateral flow membrane for the AMH LFIA.

3.5. AMH LFIA performance

To determine the analytical LOD, accuracy, and precision of the optimized AMH LFIA prototype, Calibrators A-F (cat no. AMH/MIS-CAL-105-Set; lot no. 120417; 0–15.6 ng/ml AMH), and the AMH/MIS Control Set (cat no. AL-CTR-105-SET, lot no. 120417-2020-12-03) were tested. Dipsticks were imaged and analyzed automatically in the ESEQuant LR3 reader using Lateral Flow Studio. The data was then fitted to a linear trend line to generate a regression model (Fig. 5). We determined LOD as the concentration of Calibrator C (0.41 ng/ml), as it had an average output ($\frac{TL}{CL}$) above the mean plus three standard deviations of the no-target reaction (Calibrator A). The calibration curve had an R^2 value of 0.995, indicating AMH LFIA has a linear range from 0.41 to 15.6 ng/ml of AMH.

For each calibrator the standard deviation of $\frac{TL}{CL}$ was calculated, divided by the average $\frac{TL}{CL}$, and multiplied by 100 to calculate the coefficient of variation (CV). Assay reproducibility, defined as the average coefficient of variation for the complete set of Calibrators, was estimated at 7.4%.

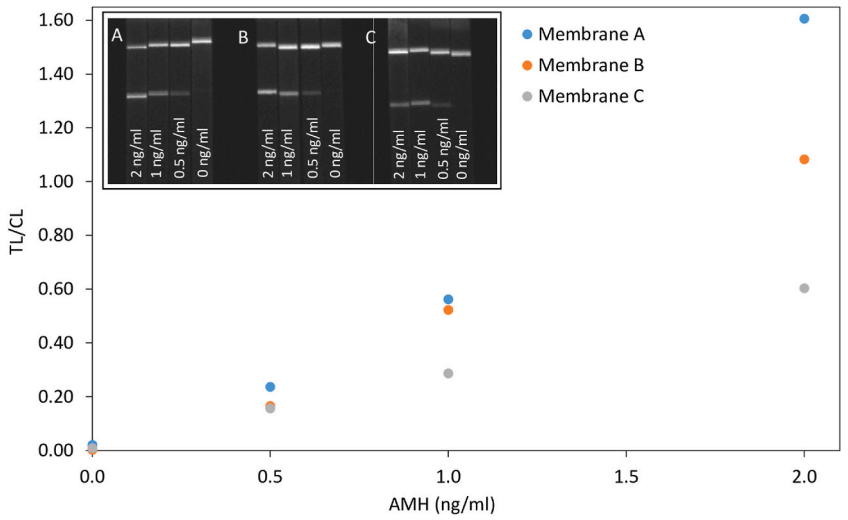

Fig. 4. Effect of nitrocellulose membrane selection on AMH LFIA. A dilution series of AMH standard (AMH/MIS Calibrator F; 14.2 ng/ml diluted to 0–2 ng/ml) was tested in AMH LFIA with dipsticks made of different nitrocellulose membranes (Membrane A: Whatman GE Healthcare FF80HP; Membrane B: Sartorius Stedim Biotech UniSart CN 95; Membrane C: Millipore HiFlow 90). The inset shows dipsticks with Membrane A (left), B (middle), and C (right) arranged in order of increasing AMH concentration and imaged on the FluorChem device (exposure 250 ms; binning of 2x2). The output ($\frac{TL}{CL}$) generated from these dipsticks was plotted as a function of AMH concentration.

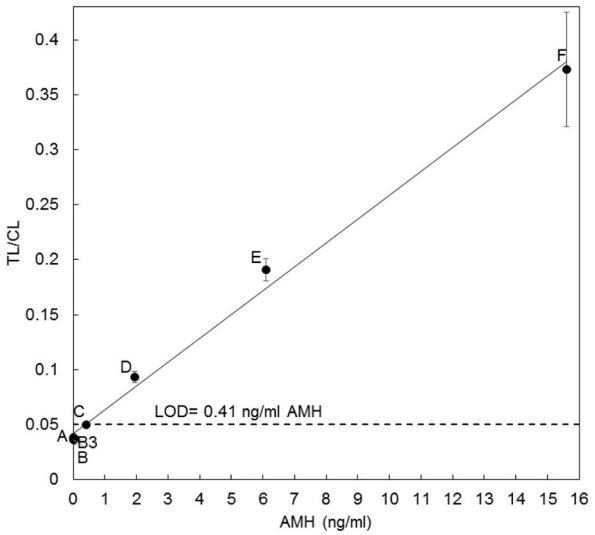

Fig. 5. AMH LFIA calibration curve obtained in ESEQuant LR3 Reader using Calibrators A-F (lot no. 120417, 0–15.6 ng/ml AMH). For each calibrator the average output ($\frac{TL}{CL}$; n = 5) was plotted against AMH concentration. The limit of detection (LOD; dotted line) was chosen as the concentration of Calibrator C (0.41 ng/ml), as it had an average output ($\frac{TL}{CL} = 0.05$) above the mean plus three standard deviations of the no-target reactions (Calibrator A, $\frac{TL}{CL} = 0.038$).

AMH Controls I and II were used to determine assay precision and accuracy in quantifying AMH concentration. The calibration curve was used to estimate the AMH concentration of Controls I and II (Table 2). We evaluated assay accuracy by the percent recovery of Control I (126%) and Control II (103%). Percent recovery was calculated by dividing the estimated over the expected AMH concentration, then multiplied by 100. We evaluated assay precision by the CV of Control I at 2.18% and II at 3.61% (n = 5; Table 2).

To accurately assess ovarian reserve in women aged 35 years and younger, AMH must be measured quantitatively at levels below 1 ng/ml since an AMH level of 1 ng/ml has been previously identified as the threshold cut-off for low ovarian reserve. Our AMH LFIA prototype showed a high degree of precision and an estimated LOD of 0.41 ng/ml, suggesting that the AMH LFIA will be able to distinguish between women with low (<0.5 ng/ml of AMH), and women with normal (0.5–4 ng/ml of AMH) ovarian reserve. A more definitive assessment of the diagnostic potential of the technology, however, will require extensive testing with clinical samples.

The calibration curve (shown in Fig. 5) and the average test output are used to calculate the observed concentration of Control I & II. The coefficient of variation (CV) was calculated by dividing the standard deviation (SD) over the mean strip output (n = 5).

4. Discussion

We present the systematic development and initial evaluation of a one-step Fluorescence Lateral Flow Immunoassay (LFIA) prototype for the detection of Anti-Müllerian Hormone (AMH). This proof-of concept study of the AMH LFIA showed a limit of detection of 0.41 ng/ml of AMH, suggesting potential clinical utility, though thorough testing with clinical samples is required to assess the true diagnostic potential of the technology. We also present a detailed workflow useful to workers interested in the development of POC LFIA tests.

The newly-developed AMH LFIA, as expected, is not as sensitive as central laboratory assays, (Table 3). However, the AMH LFIA is portable and of low complexity, and thus useable in resource-limited settings, such as a general care physician's office or a clinic. It also supports immediate testing of single samples. Point-of-care (POC), clinic-based AMH testing would make measuring one's AMH more accessible and convenient with quicker turnaround times and increased patient satisfaction. It is noteworthy that late in 2022, the American Association of Clinical Chemistry Academy revised the reproductive testing section of the *Laboratory Medicine Practice Guidelines: Evidence-Based Practice for Point-of-Care Testing.* Although no POC recommendation was made specifically for AMH testing, the updated recommendations on the utility of POC testing in the assessment of ovulation (luteinizing hormone home testing), pregnancy and premature rupture of membranes, reflect the fact that "*usage, acceptance, and even preference for point-of-care testing for a variety of conditions is surging*" [30]. The latter is also evidenced by the increasing number of online advertisements for home rapid tests, including those requiring the one-time purchase of a small home reader.

Table 2
AMH Controls I & II were tested with the optimized AMH LFIA in the ESEQuant LR3 Lateral Flow Reader (n = 5).

Sample	Expected Conc. (ng/ml)	Observed Conc. (ng/ml)	% Recovery	% CV
Control I	1.52	1.92	126	2.18
Control II	4.14	4.25	103	3.61

Table 3
Comparison of AMH LFIA to commercially available anti-Mullerian Hormone Assays.

Assay	Format	LoD	LoQ	Range	Transport/ Shipping	Incubation Time	Complexity Level
AMH LFIA	LFA	0.41 ng/ml	0.41 ng/ml	0.41–15.6 ng/ml	NO	25 min	Low
Beckman Coulter AMH Access [1,32]	magnetic particle chemiluminescence immunoassay *fully automated*	0.02 ng/ml	0.08 ng/ml	0.08–24 ng/ml	YES	40 min	High
Roche AMH Elecsys [33]	Magnetic particle chemiluminescent ELISA *fully automated*	0.01 ng/ml	0.03 ng/ml	0.03–23.0 ng/ml	YES	18 min	High
Biomerieux AMH VIDAS [33]	Fluorescent ELFA *fully automated*	0.02 ng/ml	0.06 ng/ml	0.02–9.0 ng/ml	YES	35 min	High

Moreover, point-of-care LFIAs, as compared to central-lab testing, lead to significant reductions in both testing time (sample-to-result time is typically 20–30 min for an LFIA; fully automatable ELISA run times can be less than 30 min but due to their large capacity they usually require the collection/storage of many samples for each run and do not allow for immediate testing of an individual patient) and in costs associated with transport, storage (transport/storage may also affect the stability of AMH), establishment of laboratory structures, training and supply-chain management [31]. A rapid, clinic-based AMH test could also increase the accessibility of fertility testing in developing countries, where there is a lack of access to reproductive technologies.

In addition, the AMH LFIA demonstrated a wide linear range, suggesting potential utility in the detection of other health conditions such as polycystic ovarian syndrome (PCOS) which requires AMH measurement at high concentrations (>6 ng/ml); a recent study suggests that high levels of AMH induce the development of PCOS [1], the main cause of female infertility. Conveniently screening for high AMH levels at the doctor's office could allow for more efficient detection and treatment of PCOS, or prompt referral to specialist care.

Beyond human health, rapid point-of-care AMH testing could help animal shelters non-invasively distinguish spayed and unspayed females in cat and dog populations [34,35]. The AMH LFIA also could readily be modified for AMH detection in threatened/endangered species to optimize breeding management decisions and IVF treatment [36]. Several companies have developed anti-AMH antibodies with affinity and specificity for species-specific variants of AMH (Bovine, Canine, Equine, Feline, Ovine, Primate, Rat, Mouse by Ansh Labs and Abcam; overall amino acid sequence homology between the pro-regions of different species varies from 37 to 89%).

Funding

This work was supported in part by the National Institutes of Health [1R01AR072742-01 and 1R61AI174294-01], by the DOD CDMRP [W81XWH-21-1-0975] and by the FEMSA Foundation. The funders had no role in study design, data collection and analysis, decision to publish, or preparation of the manuscript.

Author statement

Conceptualization: HJG, RCW; **Data curation/analysis:** HJG, BVV, KK, RCW; **Funding acquisition:** RCW; **Experimental Investigation:** HJG, BVV, KW, KB, KK, RCW; **Resources:** KA, AK, GS, BK, GS; **Supervision:** RCW; **Writing – original draft:** HJG, KK, RCW; **Writing – review & editing:** HJG, BVV, KW, KB, KK, KA, AK, GS, BK, GS, RCW.

Declaration of competing interest

Kannan Alpadi, Ajay Kumar, Gopal Savjani, and Bhanu Kalra are staff members of Ansh Labs, which assisted in providing AMH reagents to develop the AMH LFIA. Ansh Labs also produced the anti-AMH monoclonal antibodies and characterized AMH epitopes on the associated homodimer of AMH. The other authors have no conflict of interest to report in relation to the published work.

Data availability

Data will be made available on reasonable request.

Acknowledgments

We gratefully acknowledge financial support from the National Institutes of Health [1R01AR072742-01 and 1R61AI174294-01], the DOD CDMRP [W81XWH-21-1-0975] and the FEMSA Foundation. In addition, we would like to thank Lina Vo for her help in manuscript preparation.

References

[1] J. Bedenk, E. Vrtačnik-Bokal, I. Virant-Klun, The role of anti-Müllerian hormone (AMH) in ovarian disease and infertility, J. Assist. Reprod. Genet. 37 (2020) 89–100.
[2] H.W.R. Li, D.M. Robertson, C. Burns, W.L. Ledger, Challenges in measuring AMH in the clinical setting, Front. Endocrinol. 12 (2021), 691432.
[3] A. Abbara, et al., Anti-Müllerian hormone (AMH) in the diagnosis of menstrual disturbance due to polycystic ovarian syndrome, Front. Endocrinol. 10 (2019) 656.
[4] B. Leader, V.L. Baker, Maximizing the clinical utility of antimüllerian hormone testing in women's health, Curr. Opin. Obstet. Gynecol. 26 (2014) 226–236.
[5] N. di Clemente, C. Racine, A. Pierre, Taieb, J. Anti-Müllerian hormone in female reproduction, Endocr. Rev. 42 (2021) 753–782.
[6] F.R. Tehrani, F. Firouzi, S. Behboudi-Gandevani, Investigating the clinical utility of the anti-mullerian hormone testing for the prediction of age at menopause and assessment of functional ovarian reserve: a practical approach and recent updates, Aging Dis 13 (2022) 458–467.
[7] S.M. Nelson, et al., Two new automated, compared with two enzyme-linked immunosorbent, antimüllerian hormone assays, Fertil. Steril. 104 (2015) 1016–1021, e6.
[8] R. Punchoo, S. Bhoora, Variation in the measurement of anti-Müllerian Hormone - what are the laboratory issues? Front. Endocrinol. 12 (2021), 719029.
[9] Å. Magnusson, G. Oleröd, A. Thurin-Kjellberg, C. Bergh, The correlation between AMH assays differs depending on actual AMH levels, Hum. Reprod. Open 4 (2017)1-5.
[10] O. Rustamov, et al., Anti-Mullerian hormone: poor assay reproducibility in a large cohort of subjects suggests sample instability, Hum. Reprod. 27 (2012) 3085–3091.
[11] Y.-X. Fu, H. Wang, T. Hu, F.-M. Wang, R. Hu, Factors affecting the accuracy and reliability of the measurement of anti-Müllerian hormone concentration in the clinic, J. Int. Med. Res. 49 (2021), 3000605211016161.
[12] L. Melado, et al., Anti-müllerian hormone during natural cycle presents significant intra and intercycle variations when measured with fully automated assay, Front. Endocrinol. 9 (2018) 686.
[13] L. Khelifa, Y. Hu, N. Jiang, A.K. Yetisen, Lateral flow assays for hormone detection, Lab Chip 22 (2022) 2451–2475.
[14] S. Wang, et al., Advances in addressing technical challenges of point-of-care diagnostics in resource-limited settings, Expert Rev. Mol. Diagn. 16 (2016) 449–459.
[15] S.K. Vashist, P.B. Luppa, L.Y. Yeo, A. Ozcan, J.H.T. Luong, Emerging technologies for next-generation point-of-care testing, Trends Biotechnol. 33 (2015) 692–705.
[16] B.-S.L. Maslow, M. Guarnaccia, D. Hennessy, J.U. Klein, Age-based interpretation of anti-mullerian hormone (AMH) levels in non-infertile women [37J], Obstet. Gynecol. 133 (2019) 117S–118S.
[17] H. Zheng, et al., Ovarian response prediction in controlled ovarian stimulation for IVF using anti-Müllerian hormone in Chinese women, Medicine (Baltim.) 96 (2017) e6495.
[18] A. Revelli, et al., IVF results in patients with very low serum AMH are significantly affected by chronological age, J. Assist. Reprod. Genet. 33 (2016) 603–609.
[19] C. Ficicioglu, P.O. Cenksoy, G. Yildirim, C. Kaspar, Which cut-off value of serum anti-Müllerian hormone level can predict poor ovarian reserve, poor ovarian response to stimulation andin vitrofertilization success? A prospective data analysis, Gynecol. Endocrinol. 30 (2014) 372–376.
[20] V. Grisendi, E. Mastellari, A. La Marca, Ovarian reserve markers to identify poor responders in the context of Poseidon classification, Front. Endocrinol. 10 (2019) 281.
[21] M. Roque, T. Haahr, S.C. Esteves, P. Humaidan, The POSEIDON stratification - moving from poor ovarian response to low prognosis, JBRA Assist. Reprod. 25 (2021) 282–292.
[22] A.E. Urusov, A.V. Zherdev, B.B. Dzantiev, Towards lateral flow quantitative assays: detection approaches, Biosensors (Basel). 2019 Jul 17;9(3):89. doi: 10.3390/bios9030089.
[23] J.D. Bishop, H.V. Hsieh, D.J. Gasperino, B.H. Weigl, Sensitivity enhancement in lateral flow assays: a systems perspective, Lab Chip 19 (2019) 2486–2499.
[24] T. Salminen, E. Juntunen, S.M. Talha, K. Pettersson, High-sensitivity lateral flow immunoassay with a fluorescent lanthanide nanoparticle label, J. Immunol. Methods 465 (2019) 39–44.
[25] E.M. Linares, L.T. Kubota, J. Michaelis, S. Thalhammer, Enhancement of the detection limit for lateral flow immunoassays: evaluation and comparison of bioconjugates, J. Immunol. Methods 375 (2012) 264–270.
[26] S. Natarajan, E. Saatçi, J. Joseph, Development and evaluation of Europium-based quantitative lateral flow immunoassay for the chronic kidney disease marker Cystatin-C, J. Fluoresc. 32 (2022) 419–426.
[27] D. Dewailly, et al., The physiology and clinical utility of anti-Müllerian hormone in women, Hum. Reprod. Update 20 (2014) 370–385.
[28] L. Hu, et al., Selection and characterisation of bioreceptors to develop nanoparticle-based lateral-flow immunoassays in the context of the SARS-CoV-2 outbreak, Lab Chip 22 (2022) 2938–2943.
[29] L.A. Cantarero, J.E. Butler, J.W. Osborne, The adsorptive characteristics of proteins for polystyrene and their significance in solid-phase immunoassays, Anal. Biochem. 105 (1980) 375–382.
[30] J.A. Miller, New Guidance on Point-of-Care Testing for Reproductive Health, Clinical Laboratory News, 2022, 12-1.
[31] C.S. Kosack, A.-L. Page, P.R. Klatser, A guide to aid the selection of diagnostic tests, Bull. World Health Organ. 95 (2017) 639–645.
[32] G. Demirdjian, et al., Performance characteristics of the Access AMH assay for the quantitative determination of anti-Müllerian hormone (AMH) levels on the Access* family of automated immunoassay systems, Clin. Biochem. 49 (2016) 1267–1273.
[33] E. Pastuszek, et al., New AMH assay allows rapid point of care measurements of ovarian reserve, Gynecol. Endocrinol. 33 (2017) 638–643.
[34] N.J. Place, et al., Measurement of serum anti-Müllerian hormone concentration in female dogs and cats before and after ovariohysterectomy, J. Vet. Diagn. Invest. 23 (2011) 524–527.
[35] N.J. Place, J.-L. Cheraskin, B.S. Hansen, Evaluation of combined assessments of serum anti-Müllerian hormone and progesterone concentrations for the diagnosis of ovarian remnant syndrome in dogs, J. Am. Vet. Med. Assoc. 254 (2019) 1067–1072.
[36] P. Comizzoli, M.A. Ottinger, Understanding reproductive aging in wildlife to improve animal conservation and human reproductive health, Front. Cell Dev. Biol. 9 (2021), 680471.